

Chapter 24

A Simpler Formulation for Effective Mass Calculated from Experimental Free Mode Shapes of a Test Article on a Fixture

Randall L. Mayes and Patrick S. Hunter

Abstract Effective mass for a particular mode in a particular direction is classically calculated using a combination of fixed base mode shapes, the mass matrix, and a rigid body mode shape from a finite element model. Recently, an experimental method was developed to calculate effective mass using free experimental mode shapes of a structure on a fixture (the base) along with the measured mass of the fixture and of the test article. The method required three steps. The first step involved constraining all the free modes of the fixture except one rigid body mode in the direction of interest. The second step involved calculating pseudo-modal participation factors for this case. The third step involved constraining the final fixture rigid body degree of freedom and utilizing the constraint matrices with pseudo-modal participation factors to obtain the estimate of the standard modal participation factors which can be converted to effective mass. This work provides a simpler formulation. After the constraint in step one above, the effective masses are calculated directly from the mass normalized mode shapes of the fixture. In most cases this method gives the same answer as the original approach, within experimental error. In some instances, it appears more robust with low signal to noise ratios. It also provides better physical insight as to which modes have significant effective mass in a particular direction. The new approach is illustrated by experimental example.

Keywords Effective mass • Experimental method • Modal participation factor • Fixed base modes • Drive point FRF

Abbreviations

DoF	Degree of freedom
DP	Drive point
FRF	Frequency response function
PMPF	Pseudo-modal participation factor
$H_{dp}(\omega)$	Drive point FRF at fixture after all fixture mode shapes except one are constrained
$m_{eff r}$	Effective modal mass for mode r
m	Mass
\ddot{x}	Acceleration in one Cartesian axis direction
q	Generalized coordinate
L	Reduction matrix applying the constraint to equations of motion
Φ	Mode shapes from free modal test of test article mounted on fixture
Θ	Mode shapes of test article and fixture after all fixture mode shapes except one are constrained
ζ	Modal damping ratio
η	Generalized coordinate for partially constrained system
ω	Angular frequency (radians/second)
Ψ	Mass normalized real mode shape matrix of the fixture
Γ	Eigenvectors resulting from constraint equations
b	Subscript for the base or fixture sensor DoF

Sandia National Laboratories is a multi-program laboratory managed and operated by Sandia Corporation, a wholly owned subsidiary of Lockheed Martin Corporation, for the U.S. Department of Energy National Nuclear Security Administration under Contract DE-AC04-94AL85000.

R.L. Mayes (✉) • P.S. Hunter

Structural Dynamics Department, Sandia National Laboratories, P.O. Box 5800 – MS0557, Albuquerque, NM 87185, USA
e-mail: rlmayes@sandia.gov; pshunte@sandia.gov

<i>fix</i>	Subscript for the fixture
<i>r</i>	Subscript for mode number
<i>res</i>	Subscript for residual effective mass of all higher modes not extracted
<i>RB</i>	Subscript for the single rigid body mode of a partially constrained system
<i>TA</i>	Subscript for the test article

24.1 Introduction and Motivation

An effective mass model is a modal model that simulates response of a test article to base input in a single coordinate direction. A representation of an effective mass model is shown in Fig. 24.1. Each modal mass is scaled so that the response force of the model on the base, caused by an enforced motion of the base, accurately represents the physical force the test article would exert upon the base fixture with the same imposed motion. Another characteristic of an effective mass modal model is that the kinetic, potential and dissipated energy in the test article is reproduced accurately by the model for a given enforced base motion. When testing parts to failure, the effective mass model is useful for quantifying the failure margin over the qualification level with energy quantities that can be calculated directly from the base input accelerations that were measured. Effective mass modal models have traditionally been developed from finite element models, often times for loads analysis to make sure payloads did not overload the payload interface, for example, on a missile.

Mayes et al. [1] developed a capability to extract experimental effective mass models from a modal test of the test article on a fixture. The modal parameters of the test article/fixture assembly are constrained using the mode shapes of the fixture to obtain an estimate of the effective mass modal model for a particular direction of interest. The derivation is quite mathematical with several steps providing little physical intuition. In this work, we offer an alternative method to one of the major steps to calculate the effective masses. Although it appears to be functionally equivalent to the previous method, it provides much more physical insight by examining the base driving point frequency response function (FRF). In a recent application it appeared to be more robust to experimental mode shape errors.

24.2 Theory

The beginning of the derivation is the same as that used in the previous pseudo-modal participation factor (PMPF) approach [1], but is included for completeness. Consider a test article mounted on a fixture, or base, as represented in Fig. 24.2.

Here we consider the test article mounted to the fixture as a free structure which is typical when a structure is supported with bungee cords or foam. The modal parameters Φ , ω_r and ζ_r are extracted from an experimental modal test with modal

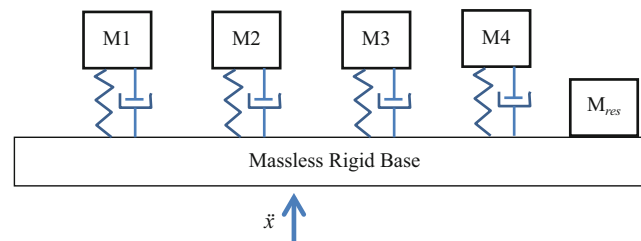
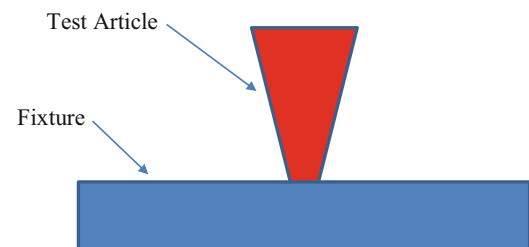


Fig. 24.1 Representation of effective mass modal model truncated to four elastic modes

Fig. 24.2 Test article on a fixture



degrees of freedom (DoF) represented as q . Mass normalized mode shapes are assumed for this derivation. Here the damping matrices are neglected for convenience, but they can be handled similarly to the mass and stiffness matrices. The free vibration modal equation of motion for the tested structure and base is

$$\left[\backslash \omega_r^2 \backslash - \omega^2 I \right] \{q\} = \{0\} \quad (24.1)$$

where the stiffness is a diagonal matrix of the squares of the natural frequencies of each mode r and the mass is a diagonal identity matrix for modal DoF vector q . There are several measurements on the base, or fixture, which will be denoted as vector x_b where subscript b denotes measurement on the base. These can be estimated from the free mode shapes, Ψ , of the base (not attached to the test article) with free base modal DoF, s , as

$$\{x_b\} \approx \Phi_b \{q\} \approx \Psi \{s\} \quad (24.2)$$

This assumes that the free mode shapes of the test article provide a set of basis vectors that accurately span the space of the base motion when the test article is attached. Because fixtures are often relatively stiff and massive with respect to the test article, sometimes the Ψ mode shapes can be extracted from the obvious fixture modes in the test article/fixture modal test to save some effort. Writing the motions in terms of base modal DoF, s , gives

$$\Psi^+ \Phi_b \{q\} \approx \{s\} \quad (24.3)$$

The requirements for instrumentation of the base fixture are that it should have enough sensors to easily determine the s DoF, which means the mode shape matrix, Ψ , should be easy to invert, i.e. have a low condition number. To provide constraints robust against experimental error, we recommend having about twice as many sensors as there are active modes of the free base fixture in the frequency band of interest. For example, consider a fixture with six rigid body modes as well as one elastic mode, such as the first twisting mode of the fixture plate. In such a case, one would have seven s DoFs and approximately 14 appropriately placed sensors would be recommended on the base to give seven independent mode shapes. The appropriate s DoFs need to be aligned perfectly with the axes in which the effective masses are desired.

In the next equations, the base motions will be constrained to zero in every s direction except the rigid body direction in which the effective mass estimates are desired. For example, assume the first s DoF is associated with the direction of interest. Therefore the $s(2:n)$ displacements would be constrained to zero by taking the second through n rows of the pseudoinverse of Ψ as

$$\Psi_{2:n}^+ \Phi_b \{q\} \approx \{s_{2:n}\} = \{0\} \quad (24.4)$$

A transformation is required to enforce the constraint. Let

$$\{q\} = L \{\eta\} \quad (24.5)$$

and substitute Eq. (24.5) into Eq. (24.4) to give

$$\Psi_{2:n}^+ \Phi_b L \{\eta\} = \{0\} \quad (24.6)$$

To guarantee that Eq. (24.6) is satisfied, L is chosen in the null space so that

$$L = \text{null}(\Psi_{2:n}^+ \Phi_b) \quad (24.7)$$

Substituting Eq. (24.5) into Eq. (24.1) and pre-multiplying by the transpose of L yields

$$L^T \left[\backslash \omega_r^2 \backslash - \omega^2 I \right] L \{\eta\} = \{0\} \quad (24.8)$$

which can be solved as an eigenvalue problem to provide modal parameters for a test article on the rigid base constrained to move only in the one direction associated with s_1 . These shapes will include one rigid body mode and $\text{length}(q) - \text{length}(s) + 1$ elastic modes. The square root of the eigenvalues from the solution of Eq. (24.8) will be the frequencies in radians/sec. If Γ

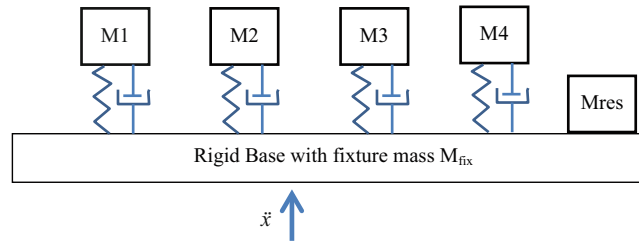


Fig. 24.3 Fixture model constrained to move only in x direction

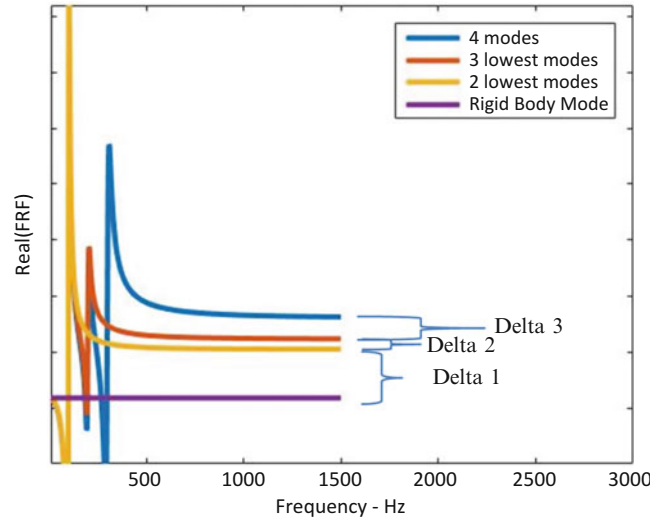


Fig. 24.4 Real part of base drive point FRF adding one mode at a time

represents the matrix of eigenvectors from solution of Eq. (24.8), the new partially constrained mode shapes of the base, Θ_b , will be

$$\Theta_b = \Phi_b L\Gamma. \quad (24.9)$$

Theoretically, the response of all DoF on the base should be the same in the axis aligned with the s_1 direction and zero in the remaining orthogonal axes. This gives a uni-directional model that looks like the effective mass model, except the base will have the mass of the fixture as shown in Fig. 24.3.

At this point the derivation deviates from the PMPF approach given previously [1]. Consider a force applied to the base of the model in Fig. 24.3 and the acceleration driving point FRF with mass normalized mode shapes as

$$H_{dp}(\omega) = \sum_{r=1}^n \frac{-\omega^2 \Theta_{br}^2}{\omega_r^2 - \omega^2 + 2j\omega\zeta_r\omega_r} \quad (24.10)$$

where Θ_{b_r} is the mode shape of the base in the x direction for mode r . Θ_{b_r} values are known from Eq. (24.9). At high frequencies in the real part of the FRF, the so-called mass lines (which are actually $1/(\text{active mass})$) are observed as modes are added to the response. At frequencies much higher than the natural frequency of one of the numbered masses in Fig. 24.3, the spring decouples the mass from the base. An example of these real valued mass lines, using the rigid body mode and three elastic modes, is given in Fig. 24.4.

The lowest amplitude mass line is associated with the one unconstrained rigid body mode (purple) and is

$$\Theta_{b_{RB}}^2 = \frac{1}{m_{fix} + m_{TA}} \quad (24.11)$$

where m_{fix} is the mass of the fixture and m_{TA} is the mass of the test article. The effective mass of the first elastic mode is associated with Delta 1 in Fig. 24.4. The larger the delta, the larger the effective mass. So the first elastic mode effective mass will be

$$m_{eff\ 1} = m_{TA+fix} - (\Phi_{b\ RB}^2 + \Phi_{b_1}^2)^{-1} = (\Phi_{b\ RB}^2)^{-1} - (\Phi_{b\ RB}^2 + \Phi_{b_1}^2)^{-1} \quad (24.12)$$

Similarly, the effective mass for any mode, r , can be calculated as

$$m_{eff\ r} = \left(\Phi_{b\ RB}^2 + \sum_{i=1}^{r-1} \Phi_{b_i}^2 \right)^{-1} - \left(\Phi_{b\ RB}^2 + \sum_{i=1}^r \Phi_{b_i}^2 \right)^{-1} \quad (24.13)$$

As the mass of the fixture approaches infinity, Eq. (24.13) becomes exact, i.e. the mode shapes converge to the fixed base modes. The less massive the fixture, the more approximate is Eq. (24.13). However, for an example analytical 3 DoF system the author processed, if the mass of the fixture was more than ten times the mass of the test article, the effective mass error was less than 0.1% of the test article mass. From previous work, the accuracy of the effective mass from experimental data is not much better than 3.5% of the test article mass, so the Eq. (24.13) approximation is well within the experimental error. In all the effective mass applications the authors have worked on, the fixture mass has always been at least a factor of ten more than the test article.

The final step to estimating the effective mass model in one direction is to find the fixed base modal frequencies so that the spring stiffness (as shown in Fig. 24.3) supporting the effective masses can be calculated. The fixed base damping is also derived in this step. The process outlined in Eqs. (24.1, 24.2, 24.3, 24.4, 24.5, 24.6, 24.7, and 24.8) is repeated, though in Eq. (24.4) only the single rigid body s DoF must be constrained to zero.

As this is an experimentally based model, it should be noted that the accuracy of the mass normalized mode shapes on the fixture, the frequencies in the modal extraction, and the rigid body mode shapes are critical to an accurate estimate of the effective mass. In the upper limit, all the effective masses sum to the total mass of the test article (not including the fixture). This is a very useful check on the experimental results.

24.3 Advantages of the New Drive Point Approach

There are advantages of the new approach over the PMPF approach [1]. In the PMPF approach, the effective mass was developed from a linear combination of the pseudo-modal participation factors. The coefficient estimates were subject to errors introduced due to modal truncation for any higher modes that were not extracted. The new approach is based only on the fixture rigid body and elastic modes of interest, so it is not dependent on higher modes that are not extracted (see Fig. 24.4). For cases in which only a few modes are extracted, this should make the new approach more robust.

The second major advantage is the physical insight generated by this theory. If one has a drive point FRF near the center of gravity on the fixture, the large deltas in the real part between modes give insight as to which modes have large effective mass and which modes do not. The imaginary part of the drive point FRF will also give this similar insight, as modes with large effective mass will have larger amplitude imaginary portion peaks than modes with small amplitude peaks (assuming similar damping). The new approach is dubbed the drive point (DP) method since it is based on a drive point FRF of the system constrained to move in one axis.

24.4 Experimental Example 1

The first example comes from a structure [1] for which 28 elastic modes were extracted using the SMAC algorithm [2]. The structure is basically a 72 kg nylon beam attached to a 605 kg steel seismic mass, all suspended by soft straps yielding rigid body modes below 5 Hz. In addition to the rigid body modes, the first plate twist mode at about 1380 Hz was constrained in the s DoF of Eq. (24.4). Currently, the authors consider this the most accurate experiment they have conducted for effective mass testing. In this experiment, the effective mass errors (computed by the previous PMPF method) as compared to a validated finite element model were within about 3.5% of the total test article mass. Effective masses were calculated for the lateral soft bending direction of the beam (see Fig. 24.5).

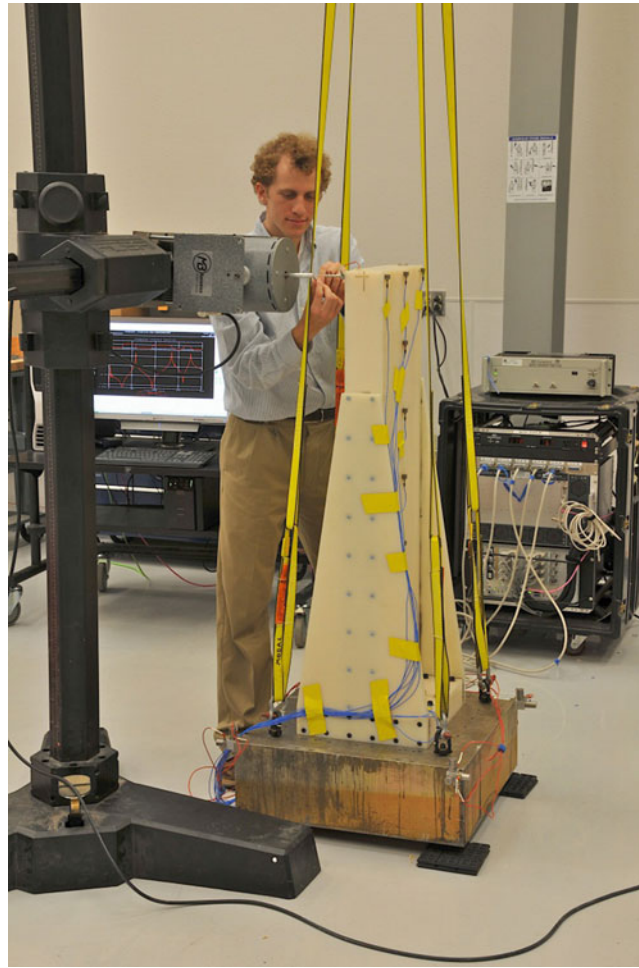


Fig. 24.5 Example 1 experimental structure for effective mass calculation

Table 24.1 Beam normalized effective masses in soft bending direction – PMPF vs new drive point theory

Fixed base test frequency (Hz)	Effective mass from PMPF	Effective mass from DP method	Difference as % of total test article mass
38	0.4152	0.4141	0.1
162	0.1870	0.1871	-0.0
393	0.0882	0.0885	-0.0
702	0.0372	0.0372	0
853	0.0036	0	0.4
1028	0.0107	0.0155	-0.5
1040	0.0031	0.0320	-2.9
1199	0.0001	0.0001	0
1301	0.0273	0.0034	2.4
1344	0.0199	0.0026	1.7
Total Mass	0.792	0.780	1.5

In Table 24.1 are provided the effective masses (normalized to 1 as the total test article mass) provided by the old PMPF method and the new DP method. All differences are less than the previously estimated worst case experimental error stated above. The final row of the table lists the sum of the effective masses, which are in good agreement for this example.

24.5 Experimental Example 2

The second example is from a project to determine effective mass from experimental data for a small component. As shown in the cut-away drawing in Fig. 24.6, the component was installed in a cavity in an aluminum fixture. The component was supported by rubber pads and held in place with a steel clamp which was secured to the fixture with cap screws. Accelerometers were placed on four of the fixture corners, several of the faces, and on the clamp. The fixture was placed on soft foam yielding rigid body modes below 30 Hz. The elastic modes were extracted using real modes in the SMAC algorithm [2]. The first unconstrained component mode was at 418 Hz and the first flexible fixture (plate twist) mode was at 3268 Hz. In addition to the rigid body modes, the plate twist mode was constrained in the s DoF of Eq. (24.4). Experimental modes were obtained and used to calculate effective masses in three orthogonal translational directions.

In Table 24.2 are provided the effective masses (normalized to 1 as the total component mass) provided by the PMPF method and the new DP method. The total effective mass is listed for each method in the last row of each section. Most of the effective mass values are consistent within 1% of the total component mass for the two methods. However, there are a few notable differences, and the sum of effective masses in the X and Y directions are more than the component mass. These issues are discussed below.

The fact that the sum of the effective masses in X and Y is more than the component mass is not physically realizable for a rigid fixture. Consider the worst case in the Y direction, where the sum of the effective mass is almost 20% greater than the component mass. There was a physical reason that led to the high effective mass estimate for the mode at 1710 Hz, which is, by itself, greater than the component mass. In the free mode shape associated with the 1710 Hz mode, there was significant Y motion of the component which also drove significant Y motion of the clamp. Therefore, the effective mass calculated at 1710 Hz included a significant percentage of the mass of the clamp as well. A rough estimate of half the mass of the active portion of the clamp participating in this mode would contribute an effective mass of 0.16 to the observed calculation. This would indicate that the effective mass of the 1710 Hz mode would be closer to 0.92 if the clamp were rigid. Although this mode had by far the most clamp motion, there was clamp motion in some of the X direction modes that would increase their effective mass as well. Since the clamp is part of the fixture, accelerometers were included on the clamp to attempt to constrain out its dynamic effects. The fixture was tested free without the component to attempt to obtain mode shapes for the clamp that could be included in the constrained s DoF of Eq. (24.4). There were three clamp modes in the empty fixture at 2161, 3776 and 3970 Hz. However, when the test article was included, these clamp modes moved to frequencies of 3276, 3969 and 4684 Hz, and their mode shapes changed significantly. When the free clamp mode shapes were included in the constraining process of Eq. (24.4), the results were disastrous with effective masses exceeding 400% of the total component mass. This suggests the free clamp mode shapes were not an adequate set of basis vectors to constrain out the true clamp motion. As such, the clamp modes were left out of the constraining process to achieve the results provided in Table 24.2.

The only large difference between the two methods was for the two modes just above 1200 Hz in the X direction. Although the effective mass sums are about the same, the individual differences are about 23% of the test article mass for those two modes, which is significant. Consider the imaginary part of the constrained driving point FRFs, H_{dp} , for each of these two modes in Fig. 24.7 below. Clearly, there is a substantial difference in their amplitudes, and correspondingly, there is an expectation for a large difference in effective mass between these two modes. For this reason, the authors believe that the

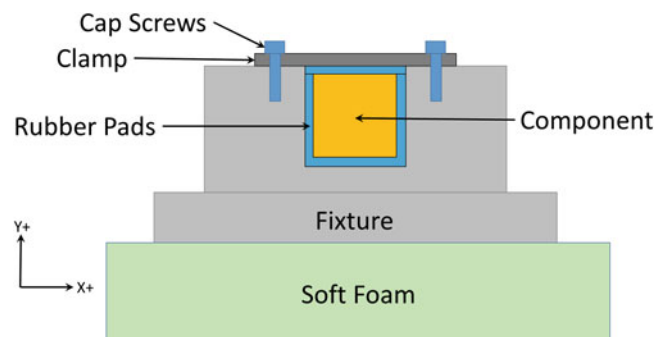
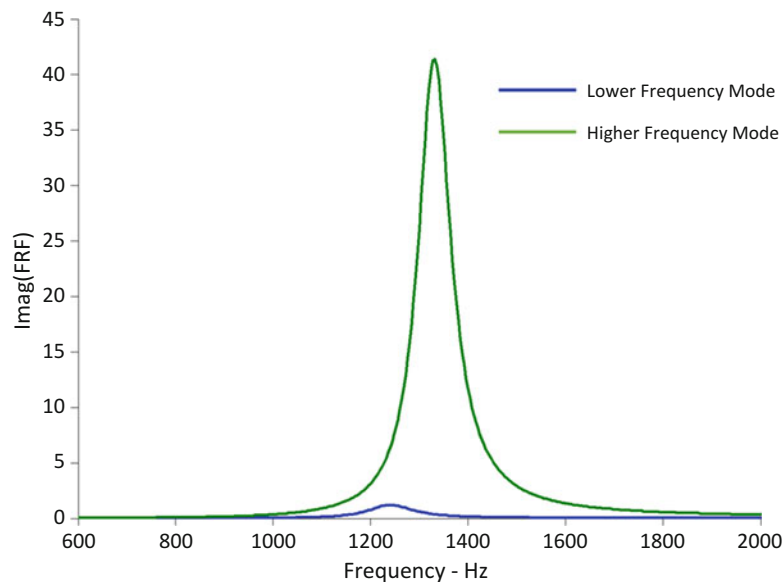


Fig. 24.6 Example 2 experimental setup for effective mass calculation

Table 24.2 Component normalized effective masses in three directions – PMPF vs new drive point theory

Fixed base frequency (Hz)	Effective mass from PMPF	Effective mass from DP method	Difference as % of total component mass
X direction			
397	0.001	0.001	0.0
644	0.111	0.105	-0.6
875	0.001	0.001	0.0
1227	0.388	0.155	-23.3
1292	0.593	0.826	23.2
1710	0.008	0.010	0.2
<u>Total Mass</u>	1.102	1.097	-0.5
Y direction			
397	0.000	0.000	0.0
644	0.007	0.007	0.0
875	0.095	0.089	-0.6
1227	0.007	0.006	-0.1
1292	0.011	0.009	-0.2
1710	1.076	1.079	0.3
<u>Total Mass</u>	1.196	1.190	-0.6
Z direction			
397	0.951	0.946	-0.5
644	0.008	0.008	0.1
875	0.000	0.000	0.0
1227	0.000	0.000	0.0
1292	0.002	0.002	0.0
1710	0.002	0.002	0.0
<u>Total Mass</u>	0.963	0.959	-0.5

**Fig. 24.7** Imaginary part of constrained drive point FRF for two modes of interest

DP estimate is more reasonable. Also, the higher mode is a translation of the component in X while the lower frequency mode is a rotation about X. It seems reasonable that the translation mode would have more effective mass in the translation direction than the rotational mode. Although this is only a single example, it may be that the DP method is demonstrating its robustness against modal truncation errors in a case where only six elastic modes of the component were extracted.

24.6 Conclusions

A revised theoretical approach, referred to as the Drive Point method, for calculating effective mass of a test article mounted on a fixture is presented with experimental examples. Effective mass experiments consist of a free modal test of the test article mounted on a fixture. When compared against the previous pseudo-modal participation factor approach on the authors' "best" previous effective mass experiment, the effective masses agreed within previously established error bounds.

The new approach provides insight from a drive point FRF at the center of gravity of the fixture, showing the large resonant responses that correspond to large effective masses for the test article. In the second experimental example, this insight was helpful in determining which approach was most appropriate where the two approaches showed significant differences. The Drive Point approach is not as prone to modal truncation error as the previous pseudo-modal participation factor approach. This is of particular advantage when there are only a few modes that can be extracted in the modal test. Although most of the effective mass estimates were nearly equivalent with the two approaches, the drive point approach appeared to give more reasonable results for X direction effective mass for two modes. This may reinforce the theoretical advantage, since the second example had many fewer modes than the first example, leading to possible modal truncation errors. In the second example, the fixture also exhibited motion of a clamp which was not able to be constrained, erroneously contributing fixture mass to some of the calculated component effective mass values.

Acknowledgement Notice: This manuscript has been authored by Sandia Corporation under Contract No. DE-AC04-94AL85000 with the U.S. Department of Energy. The United States Government retains and the publisher, by accepting the article for publication, acknowledges that the United States Government retains a non-exclusive, paid-up, irrevocable, world-wide license to publish or reproduce the published form of this manuscript, or allow others to do so, for United States Government purposes.

References

1. Mayes, R.L., Schoenherr, T.F., Blecke, J., Rohe, D.P.: Efficient method of measuring effective mass of a system. Proceedings of the 31st International Modal Analysis Conference, Garden Grove, CA, February 2013, paper #194
2. Hensley, D.P., Mayes, R.L.: Extending SMAC to multiple references. Proceedings of the 24th International Modal Analysis Conference, Orlando, FL, pp. 220–230, January 2006